Electronic Supplementary Material (ESI) for Inorganic Chemistry Frontiers.

Synthesis and structure of new binuclear ruthenium(II) arene benzil bis(benzoylhydrazone) complexes: Investigation on antiproliferative activity and apoptosis induction

Mohamed Kasim Mohamed Subarkhan,[†] Sundar Saranya,[†] and Rengan Ramesh*,[†]

[†]Centre for Organometallic Chemistry, School of Chemistry, Bharathidasan University, Tiruchirappalli 620 024, Tamil Nadu, India.

Table of the content **Page No.**

EXPERIMENTAL SECTION

Methods and Instrumentation. The microanalysis of C, H and N were recorded by an analytical function testing Vario EL III CHNS elemental analyser. Melting points were recorded with a Boetius micro-heating table and are corrected. FT-IR spectra were recorded in KBr pellets with JASCO 400 plus spectrometer. Electronic spectra in $CHCl_3$ solution were recorded with a CARY 300 Bio UV- visible Varian spectrometer. ^{1}H and ^{13}C NMR spectra were recorded on a Bruker 400 MHz instrument using tetramethylsilane (TMS) as an internal reference. ESI-MS were recorded on a Thermo Fisher Hybrid Quadrupole-Orbitrap mass spectrometer in positive ion electrospray ionization (ESI) mode. The ruthenium arene complexes content was analysed on a Thermo Scientific X-Series ICP-MS instrument.

X-ray Crystallography. Single crystals of $[Ru_2(\eta^6\text{-}C_6H_6)_2(Cl)_2(L3)]$ (**3**) and $[Ru_2(\eta^6\text{-}p\text{-}cymene)_2(Cl)_2(L1)]$ (**4**) were grown by slow evaporation of DCM-ethanol solution at RT. A single crystal of suitable size was covered with Paratone oil, mounted on the top of a glass fiber, and transferred to a Bruker AXS Kappa APEX II single crystal X-ray diffractometer using monochromated MoKα radiation (λ=0.71073). Data were collected at 173 K (**3**) and 296K (**4**). Bruker SAINT Plus (Version 7.06a) software was used to perform frame integration and data reduction. SADABS software has been used for multi scan absorption corrections. The structures were solved by intrinsic phasing (SHELXS-97)[1] and refined by full-matrix least-squares procedures on F^2 with all measured reflections SHELXL[2] program with anisotropic temperature factors for all non-hydrogen atoms. All hydrogen atoms were added geometrically and refined by using a riding model. Figure **3** and **4** were drawn with ORTEP[3] and the structural data deposited at The Cambridge Crystallographic Data Centre: CCDC **1520810** and **1520809.**

Partition Coefficients Determination. The hydrophobicity values of the complexes **1-6** were measured by the "Shake flask" method in octanol - water phase partitions as reported earlier. Complexes **1-6** (1 mg/mL) were dissolved in a mixture of water and *n*-octanol (2, 4, 6, 8, 10 μg/mL) followed by shaking for 1 hour. The mixture was allowed to settle over a period of 30 minutes and the resulting two phases were collected separately without cross contamination of one solvent layer into another. The concentration of the complexes in each phase was determined by UV-Vis absorption spectroscopy at room temperature. The results are given as the mean values obtained from three independent experiments. The log *P* was calculated using sample solution

concentration. Partition coefficients for **1-6** were calculated using the equation log *P* = log[(**1-6**)oct/(**1-6**)aq].

Cell Culture and Inhibition of Cell Growth.

Cell Culture. HeLa (human cervical cancer cell line), MDA-MB-231 (Triple negative breast carcinoma), Hep G2 (human liver carcinoma cell line) and NIH 3T3 (noncancerous cell, mouse embryonic fibroblast)were obtained from the National Centre for Cell Science (NCCS), Pune. These cell lines were cultured as a monolayer in RPMI-1640 medium (Biochrom AG, Berlin, Germany), supplemented with 10% fetal bovine serum (Sigma-Aldrich, St. Louis, MO, USA) and with 100 U mL^{-1} penicillin and 100 µg mL^{-1} streptomycin as antibiotics (Himedia, Mumbai, India), at 37 ^{o}C in a humidified atmosphere of 5% CO_2 in a CO_2 incubator (Heraeus, Hanau, Germany).

Bioassays. For the biological examination (cytotoxicity), the complexes and corresponding ligands were dissolved in DMSO (20 mM) prior to use. DMSO solutions were mixed with the aqueous solutions used in biological studies immediately prior to use, so that the final concentration of DMSO never exceeded 0.1% (v/v).

Inhibition of Cell Growth. The IC_{50} values, which are the concentrations of the tested compounds that inhibit 50% of cell growth, were determined using a 3-(4,5-dimethyl thiazol-2yl)-2,5-diphenyl tetrazolium bromide (MTT) assay. Cells were plated in their growth medium at a density of 5000 cells per well in 96 flat bottomed well plates. After 24 h plating, benzoylhydrazone ligands and the binuclear Ru(II) arene benzoylhydrazone complexes **1-6** were added at different concentrations for 24 h to study the dose dependent cytotoxic effect. To each well, 20 µL of 5 mg mL^{-1} MTT in phosphate-buffer (PBS) was added. The plates were wrapped with aluminium foil and incubated for 4 h at 37 ˚C. The purple formazan product was dissolved by addition of 100 µL of 100% DMSO to each well. The quantity of formazan formed gave a measure of the number of viable cells. HeLa, MDA-MB-231and Hep G2 were used for the MTT assay. The absorbance was monitored at 570 nm (measurement) and 630 nm (reference) using a 96 well plate reader (Bio-Rad, Hercules, CA, USA). Data were collected for four replicates each and used to calculate the respective means. The percentage of inhibition was calculated, from this data, using the formula: Percentage inhibition = 100 x {Mean OD of untreated cells (control) – Mean OD of treated cells} /{Mean OD of untreated cells

(control)}. The IC_{50} value was determined as the complex concentration that is required to reduce the absorbance to half that of the control.[4]

Acridine Orange and Ethidium Bromide Staining Experiment. The changes in chromatin organization in MDA-MB-231 cells after treatment with IC_{50} concentration of the complexes **4** and **6** by using acridine orange (AO) and ethidium bromide (EB). Briefly, about 5 x 10^5 cells were allowed to adhere overnight on a coverslip placed in each well of a 6-well plate. The cells were allowed to recover for 1 h, washed thrice with DPBS, stained with an AO and EB mixture (1:1, 10 μM) for 15 min, and observed with epifluorescence microscope (Carl Zeiss, Germany).[5]

Hoechst 33258 Staining Method. Hoechst 33258 staining was done using the method described earlier with slight modifications. 5×10^5 MDA-MB-231 cells were treated with IC_{50} concentration of the complexes **4** and **6** for 24 h in a 6-well culture plate and were fixed with 4% paraformaldehyde followed by permeabilization with 0.1% Triton X-100. Cells were then stained with 50 μg mL^{-1} Hoechst 33258 for 30 min at room temperature. The cells undergoing apoptosis, represented by the morphological changes of apoptotic nuclei, were observed and imaged by epifluorescence microscope (Carl Zeiss, Germany).[6]

Apoptosis Evaluation - Flow Cytometry. The MDA-MB-231 cells were grown in a 6-well culture plate and exposed to IC_{50} concentrations of complexes **4** and **6** for 24 h. The Annexin V-FITC kit uses annexin V conjugated with fluorescein isothiocyanate (FITC) to label phosphatidylserine sites on the membrane surface of apoptotic cells. Briefly the cells were trypsinised and washed with Annexin binding buffer and incubated with Annexin V-FITC and PI for 30 minutes and immediately analysed using flow cytometer FACS Aria-II. The results were analysed using DIVA software and percentage positive cells were calculated.

Annexin V-FITC staining assay. MDA-MB-231 cells in culture are negative for Annexin V-FITC and negative for PI. Cells that are induced to undergo apoptosis are positive for Annexin V FITC and negative for PI. Both cells in the later stages of apoptosis and necrotic cells are positive for Annexin V-FITC and PI. Controls and samples treated with the complexes **1–6**, MDA-MB-231 cells were rinsed and washed once with 500 μl of 1 × Assay Buffer per well. Following 100 μl of Assay Buffer was added to each well, containing 1 μg of Annexin V-FITC

and 10 µl of propidium iodide. After the incubation of cells for 15 min at room temperature in the dark, the fluorescence intensity of Annexin V-FITC and of propidium iodide was evaluated with epifluorescence microscope (Carl Zeiss, Germany). Flow cytometry were used to measure the fluorescence intensity of the cells (Annexin V-FITC, λ_{ex} - 488 nm, λ_{em} - 500-560 nm; PI, λ_{ex} - 488 nm, λ_{em} - 600-680 nm).[7]

Cellular DNA Damage by the Comet Assay. DNA damage was quantified by means of the comet assay as described. Assays were performed under red light at 4 ^{o}C. Cells used for the comet assay were sampled from a monolayer during the growing phase, 24 h after seeding. MDA-MB-231 cells were treated with the complexes **4** and **6** at IC_{50} concentration, and cells were harvested by a trypsinization process at 24 h. A total of 200 µL of 1% normal agarose in PBS at 65 ^{o}C was dropped gently onto a fully frosted microslide, covered immediately with a coverslip, and placed over a frozen ice pack for about 5 min. The coverslip was removed after the gel had set. The cell suspension from one fraction was mixed with 1% low-melting agarose at 37 ^{o}C in a 1:3 ratio. A total of 100 µL of this mixture was applied quickly on top of the gel, coated over the microslide, and allowed to set as before. A third coating of 100 µL of 1% low-melting agarose was placed on the gel containing the cell suspension and allowed to set. Similarly, slides were prepared (in duplicate) for each cell fraction. After solidification of the agarose, the coverslips were removed, and the slides were immersed in an ice-cold lysis solution (2.5 M NaCl, 100 mM Na_2EDTA, 10 mM Tris, NaOH; pH 10, 0.1% Triton X-100) and placed in a refrigerator at 4 ^{o}C for 16 h. All of the above operations were performed in low-lighting conditions in order to avoid additional DNA damage. Slides, after removal from the lysis solution, were placed horizontally in an electrophoresis tank. The reservoirs were filled with an electrophoresis buffer (300 mM NaOH and 1 mM Na_2EDTA, pH > 13) until the slides were just immersed in it. The slides were allowed to stand in the buffer for about 20 min (to allow DNA unwinding), after which electrophoresis was carried out at 0.8 v cm^{-1} for 15 min. After electrophoresis, the slides were removed, washed thrice in a neutralization buffer (0.4 M Tris, pH 7.5), and gently dabbed to dry. Nuclear DNA was stained with 20 µL of EB (50 µg mL^{-1}). Photographs were taken using an epifluorescence microscope (Carl Zeiss).[8]

Mitochondrial Membrane Potential ($\Delta\psi_m$) Assay. Mitochondrial membrane potential, $\Delta\psi_m$ is an important parameter of mitochondrial function used as an indicator of cell health. MDA-MB-231 cells treated overnight with IC_{50} concentration of the complexes **4** and **6** in 6-well plates were incubated for 1 h with 2 µg mL^{-1} of JC−1 in the culture medium. The adherent cell

layer was then washed three times with PBS and dislodged with 250 µL of trypsin−EDTA. Cells were collected in PBS/2% bovine serum albumin (BSA), washed twice by centrifugation, resuspended in 0.3 mL of PBS/2% BSA, mixed gently, and examined in the fluorescent microscope (Carl Zeiss, Jena, Germany).

Western Blot Analysis. MDA-MB-231 cells were treated with the complexes **4** and **6** at IC_{50} concentration for 24 h, and appropriate amounts of cell lysates (25 µg proteins) were resolved over 10% Tris–glycine polyacrylamide gel, and then transferred onto the PVDF membrane. The blots were blocked using 5% non-fat dry milk and probed using p53, Bcl-2, and Bax in blocking buffer overnight at 4 ^{o}C. The membrane was then incubated with appropriate secondary antibody-horseradish peroxidase conjugate (Amersham Life Sciences Inc., IL, USA), followed by detection using chemiluminescence ECL kit (Amersham Life Sciences Inc., IL, USA). To ensure equal loading of protein, the membrane was stripped and reprobed with anti-b-actin antibody (Sigma Aldrich, USA).[9]

1. (a) G. Sheldrick. SHELXL-97; University of Göttingen, Göttingen, Germany, 1997. (b) G. Sheldrick, SHELXL-2013; University of Göttingen, Göttingen, Germany, 2013.

2. G. Sheldrick, *Acta Cryst. Sec. C*: *Struct. Chem*. 2015, **71**, 3-8.

3. L. Farrugia, *J. Appl. Cryst.*, 1999, **32**, 837-838.

4. M. K. Mohamed Subarkhan, R. Ramesh and Y. Liu, *New J. Chem.*, 2016, **40**, 9813-9823.

5. M. Blagosklonny and W.S. El-Diery, *Int. J. Cancer* 1996, **67**, 386.

6. G.P.A.H. Kasibhatla, D. Finucane, T. Brunner, E.B. Wetzel and D.R. Green, Protocol: Staining of suspension cells with Hoechst 33258 to detect apoptosis. Cell: A laboratory manual Culture and Biochemical Analysis of Cells; CSHL Press: Cold Spring Harbor, NY, 2000; **Vol. 1**, p 15.5.

7. A. Louie, *Chem. Rev.*, 2010, **110**, 3146-3195.

8. C.R. Sihn, E.J. Suh, K.H. Lee, T.Y. Kim and S.H. Kim, *Cancer Lett.* 2003, **201**, 203.

9. Mohamed Subarkhan, M.; Prabhu, R. N.; Raj Kumar, R.; Ramesh, R. *RSC Adv.* 2016**, 6**, 25082-25093.

Table S1. Selected crystal data and structure refinement summary of **3** and **4**.CH_2Cl_2

Complex	**3**	**4**. CH_2Cl_2
CCDC number	1520810	1520809
Chemical formula	$C_{42}H_{36}Cl_2N_4O_4Ru_2$, CH_3CH_2OH[a]	$C_{49}H_{49}Cl_4N_4O_2Ru_2$
Formula weight	933.79	1069.86
color and habit	orange, prism	red, block
Crystal system	Monoclinic	Triclinic
Space group	$P21/c$	$P\bar{1}$
Temperature (K)	173	296
a (Å)	22.1609 (7)	11.1554 (8)
b (Å)	8.6759 (3)	11.5176 (8)
c (Å)	21.5920 (7)	18.4679 (13)
α (°)	90	99.317 (2)
β (°)	95.7620(10)	95.757 (2)
γ (°)	90	98.084 (2)
Volume ($Å^3$)	4130.4 (2)	2299.8 (3)
Z	4	2
ρ (g cm^{-3})	1.502	1.545
μ (mm^{-1})	0.91	7.80
Reflections used	9939	9879
R1, wR2 [I≥ 2σ(I)]	0.0475, 0.0993	0.0380, 0.1174
Goodness-of-fit on F2	1.110	1.073

[a]The asymmetric unit also contains one ethanol (CH_3CH_2OH) solvate which was grossly disordered and was excluded using SQUEEZE subroutine in PLATON [A. L. Spek, Acta Crystallogr., Sect. D: Biol. Crystallogr., 2009, D65, 148–155].

Table S2. Selected Bond Lengths (Å) and Angles (deg) in complexes **3** and **4**. CH_2Cl_2

	3		**4**. CH_2Cl_2
Ru(1)-N(1)	2.103(2)	Ru(1)-N(1)	2.096 (2)
Ru(1)-O(1)	2.041 (2)	Ru(1)-O(2)	2.064 (2)
Ru(1)-Cl(1)	2.3872(9)	Ru(1)-Cl(1)	2.4101(8)
Ru(1)-C(32)	2.147(4)	Ru(1)-C(5)	2.202(3)
N(1)-N(2)	1.410 (3)	N(1)-N(3)	1.411 (4)
N(2)-C(15)	1.315 (4)	N(3)-C(11)	1.315 (4)
O(1)-C(15)	1.292 (3)	O(2)-C(11)	1.289 (4)
O(1)-Ru(1)-N(1)	76.64 (9)	O(2)-Ru(1)-N(1)	76.39 (9)
N(1)-Ru(1)-Cl(1)	86.15 (7)	N(1)-Ru(1)-Cl(1)	86.98 (7)
N(2)-N(1)-Ru(1)	113.85 (17)	N(3)-N(1)-Ru(1)	114.47 (18)
C(32)-Ru(1)-Cl(1)	145.62 (19)	C(11)-O(2)-Ru(1)	113.05(18)
O(1)-Ru(1)-Cl(1)	83.32 (7)	C(5)-Ru(1)-Cl(1)	92.64 (10)
C(15)-O(1)-Ru(1)	113.59(17)	O(2)-Ru(1)-Cl(1)	86.20 (6)
C(15)-N(2)-N(1)	110.9 (2)	C(11)-N(3)-N(1)	110.8 (2)
Ru(2)-N(3)	2.095(2)	Ru(2)-N(2)	2.101(3)
Ru(2)-O(3)	2.061 (2)	Ru(2)-O(3)	2.056 (2)
Ru(2)-Cl(2)	2.4040 (8)	Ru(2)-Cl(2)	2.4321 (8)
Ru(2)-C(39)	2.154 (4)	Ru(2)-C(22)	2.170 (3)
N(3)-N(4)	1.408 (3)	N(2)-N(4)	1.409 (4)
N(4)-C(23)	1.316 (4)	N(4)-C(29)	1.312 (4)
O(3)-C(23)	1.287 (4)	O(3)-C(29)	1.294 (4)
O(3)-Ru(2)-N(3)	76.47 (9)	O(3)-Ru(2)-N(2)	76.42 (9)
N(3)-Ru(2)-Cl(2)	90.31 (7)	N(2)-Ru(2)-Cl(2)	88.51 (7)
N(4)-N(3)-Ru(2)	114.03 (18)	N(4)-N(2)-Ru(2)	113.67 (18)
C(39)-Ru(2)-Cl(2)	148.06 (15)	C(29)-O(3)-Ru(2)	112.60(19)
O(3)-Ru(2)-Cl(2)	83.43 (7)	C(22)-Ru(2)-Cl(2)	117.92 (9)
C(23)-O(3)-Ru(2)	113.2(5)	O(3)-Ru(2)-Cl(2)	86.84 (6)
C(23)-N(4)-N(3)	112.65 (18)	C(29)-N(4)-N(2)	110.9 (2)

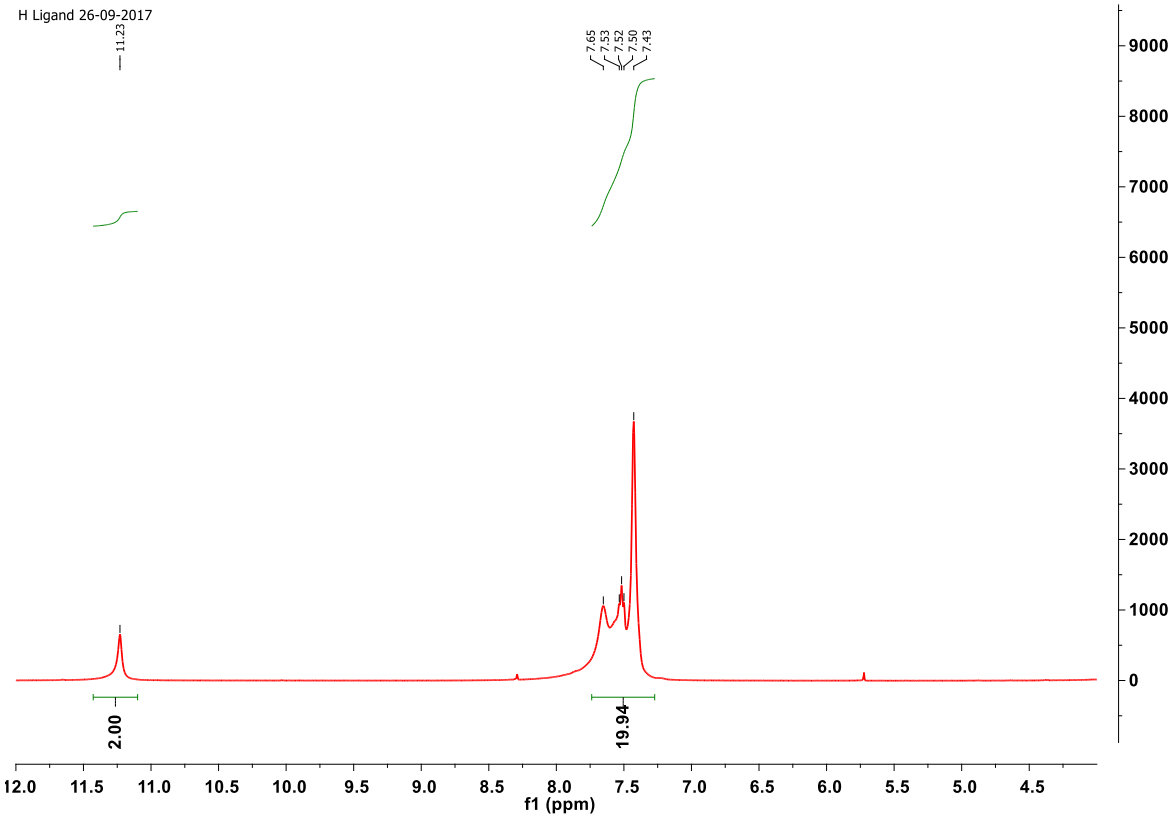

Figure S1. ^{1}H NMR spectrum of Ligand (**1**) in DMSO at 400 MHz.

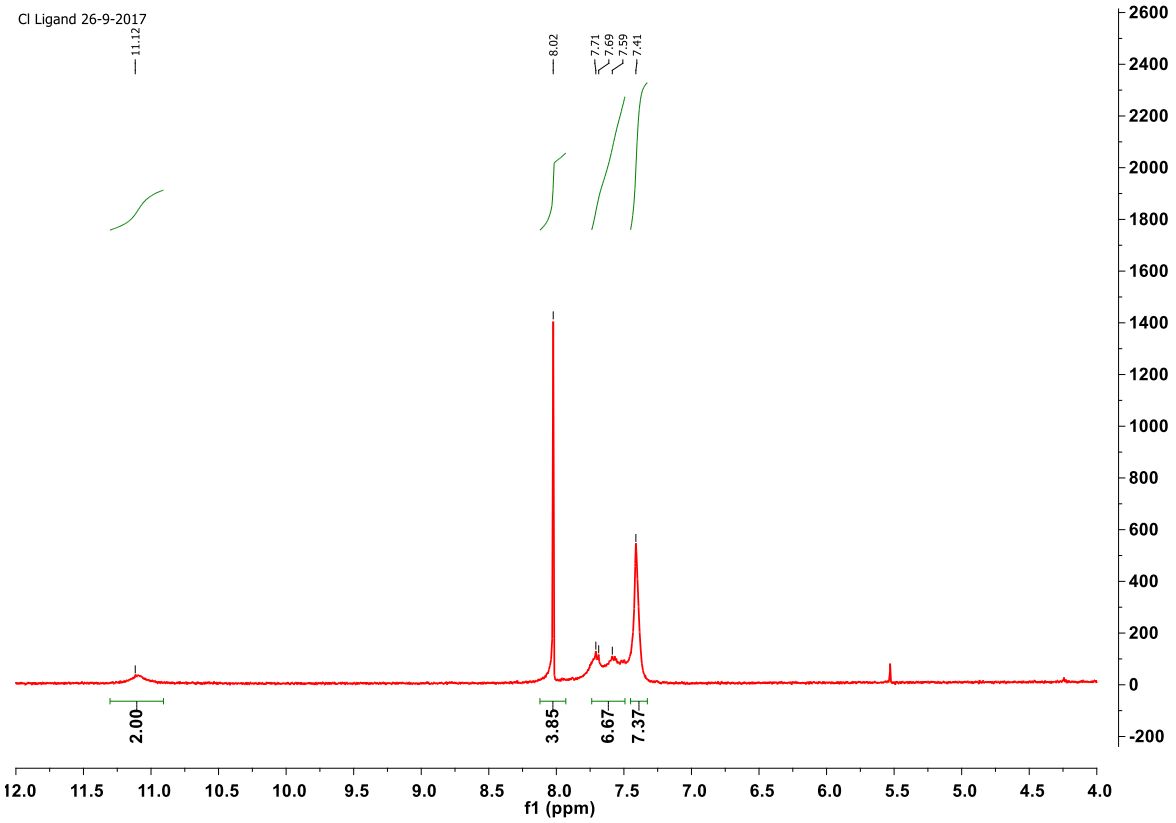

Figure S2. ^{1}H NMR spectrum of Ligand (**2**) in DMSO at 400 MHz.

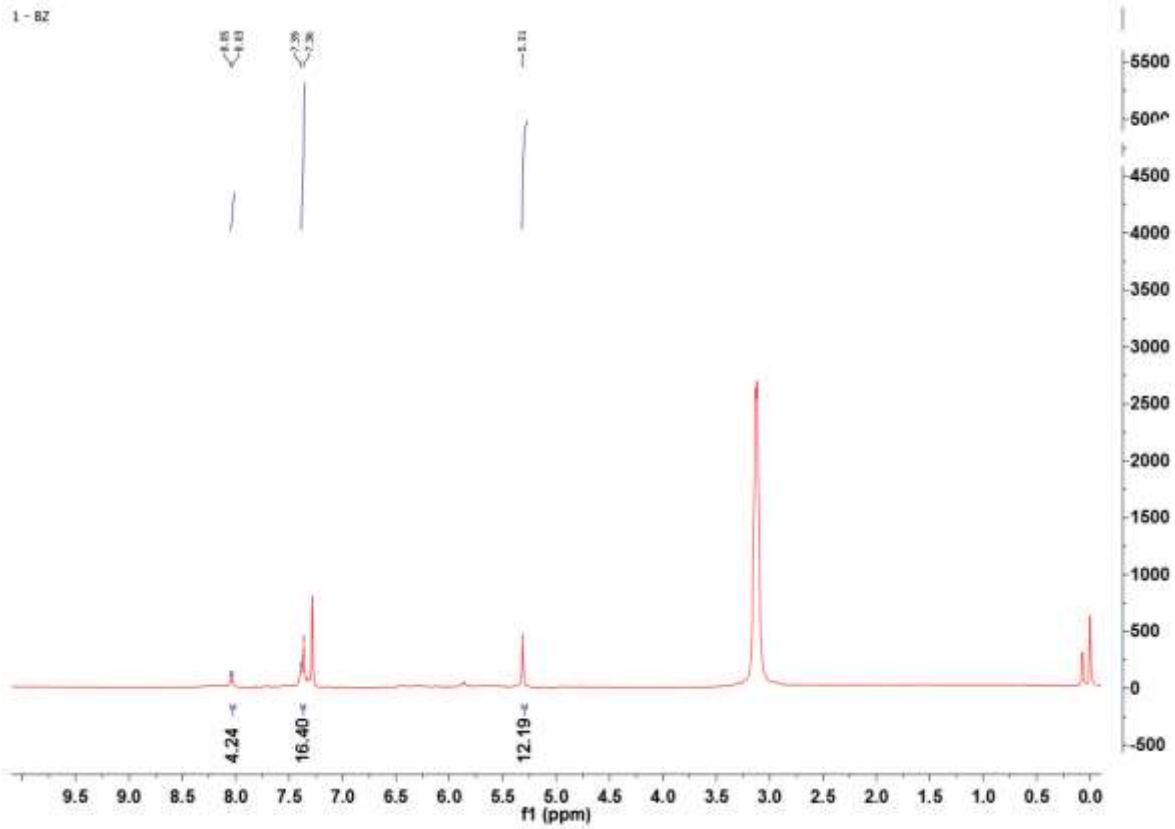

Figure S3. ^{1}H NMR spectrum of [$Ru_2(\eta^6\text{-}C_6H_6)_2(Cl)_2$(L1)] (**1**) in $CDCl_3$ at 400 MHz.

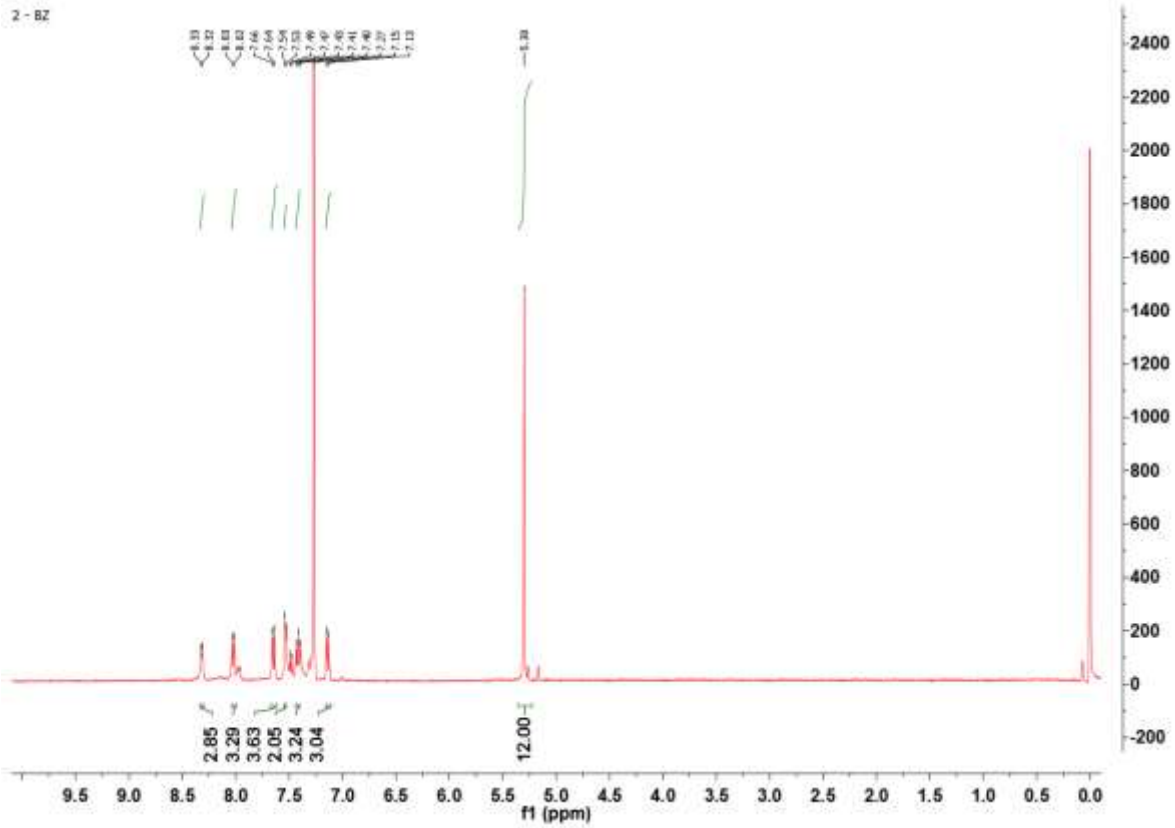

Figure S4. ^{1}H NMR spectrum of [$Ru_2(\eta^6\text{-}C_6H_6)_2(Cl)_2$(L2)] (**2**) in $CDCl_3$ at 400 MHz.

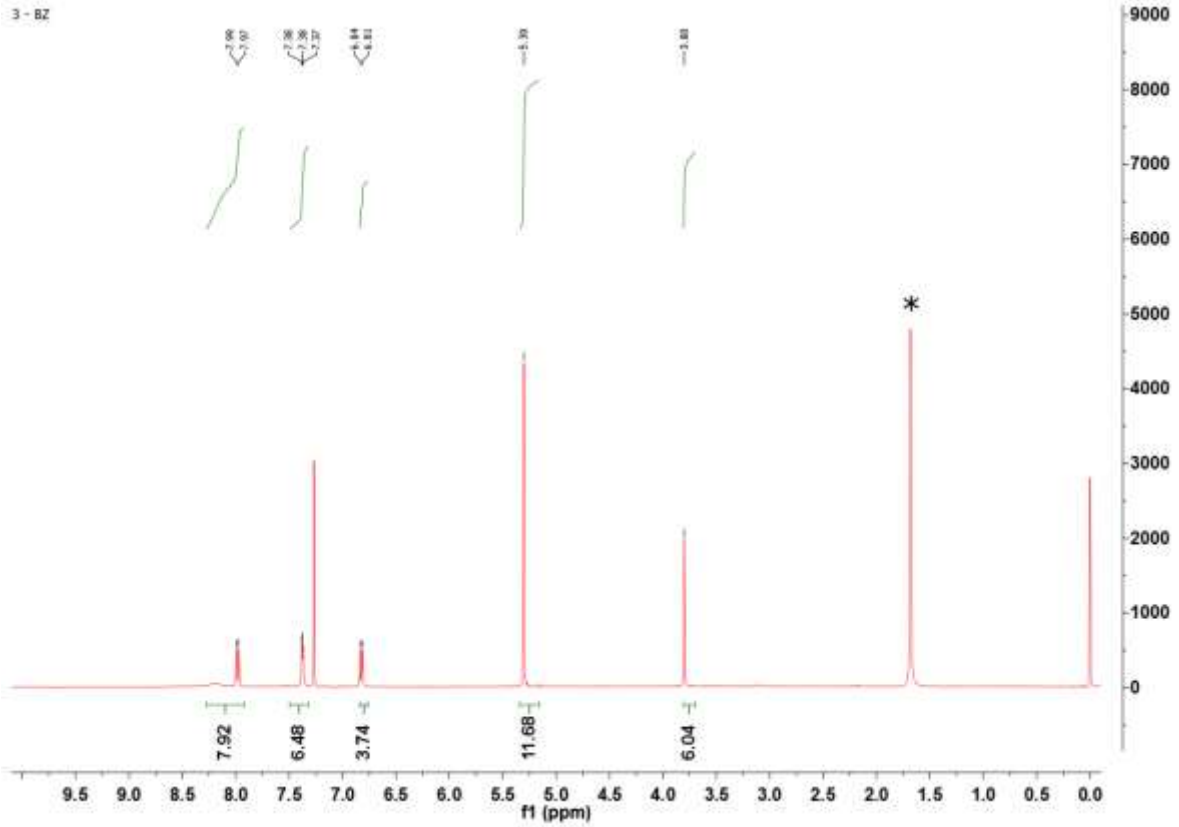

Figure S5. ^{1}H NMR spectrum of [$Ru_2(\eta^6\text{-}C_6H_6)_2(Cl)_2$(L3)] (**3**) in $CDCl_3$ at 400 MHz.

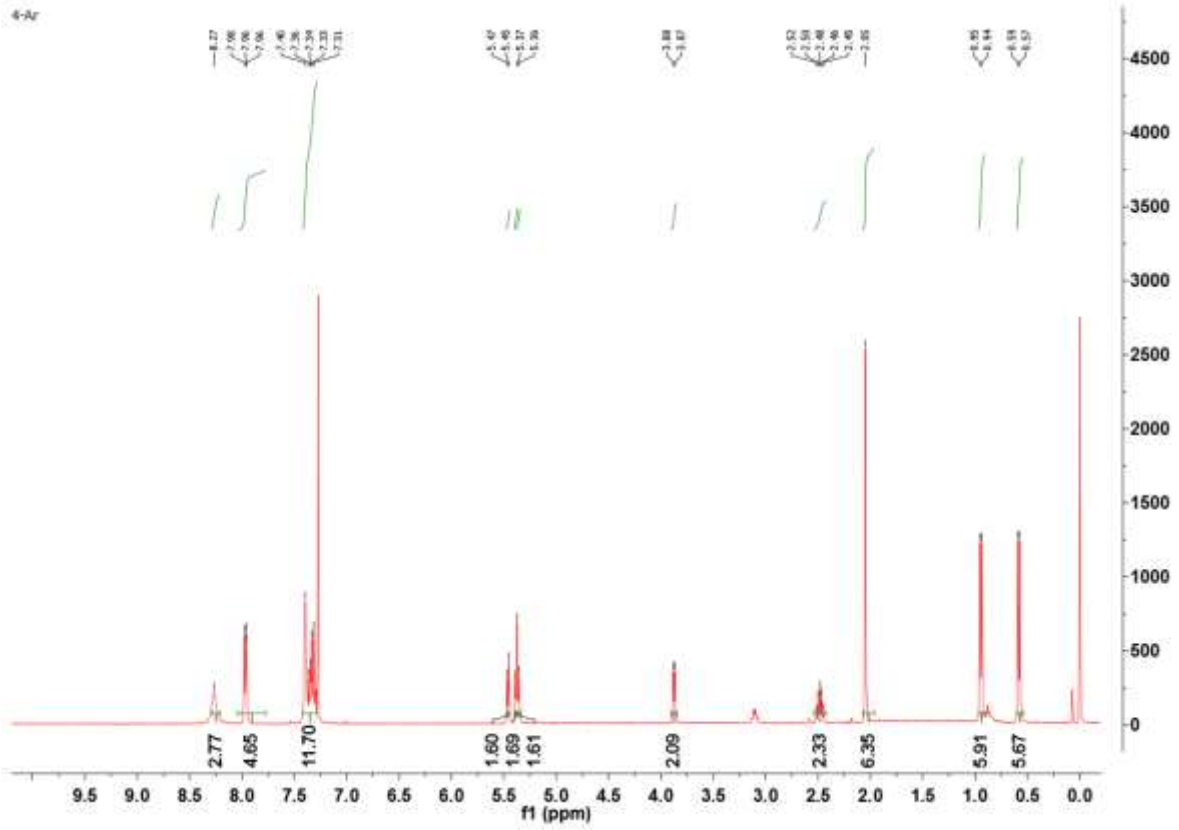

Figure S6. ^{1}H NMR spectrum of [$Ru_2(\eta^6$-p-cymene$)_2(Cl)_2$(L1)] (**4**) in $CDCl_3$ at 400 MHz.

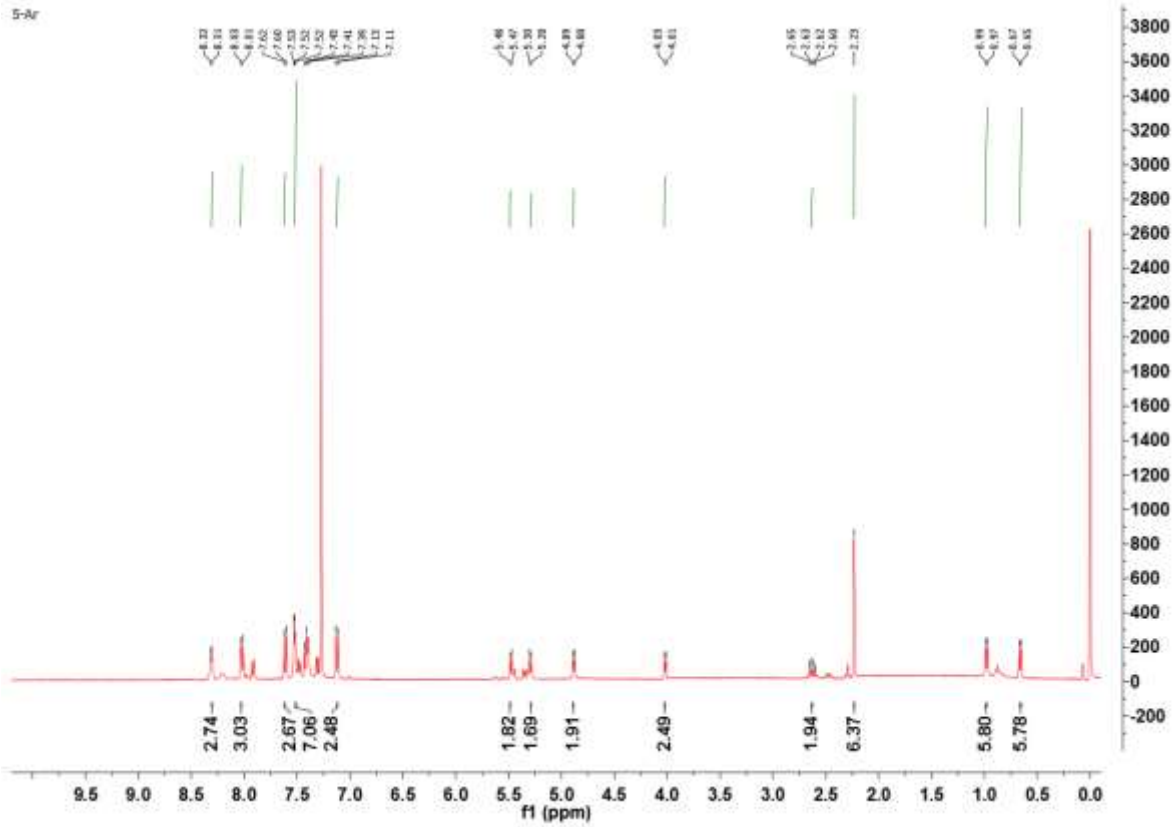

Figure S7. ^{1}H NMR spectrum of [$Ru_2(\eta^6$-p-cymene$)_2(Cl)_2$(L2)] (**5**) in $CDCl_3$ at 400 MHz.

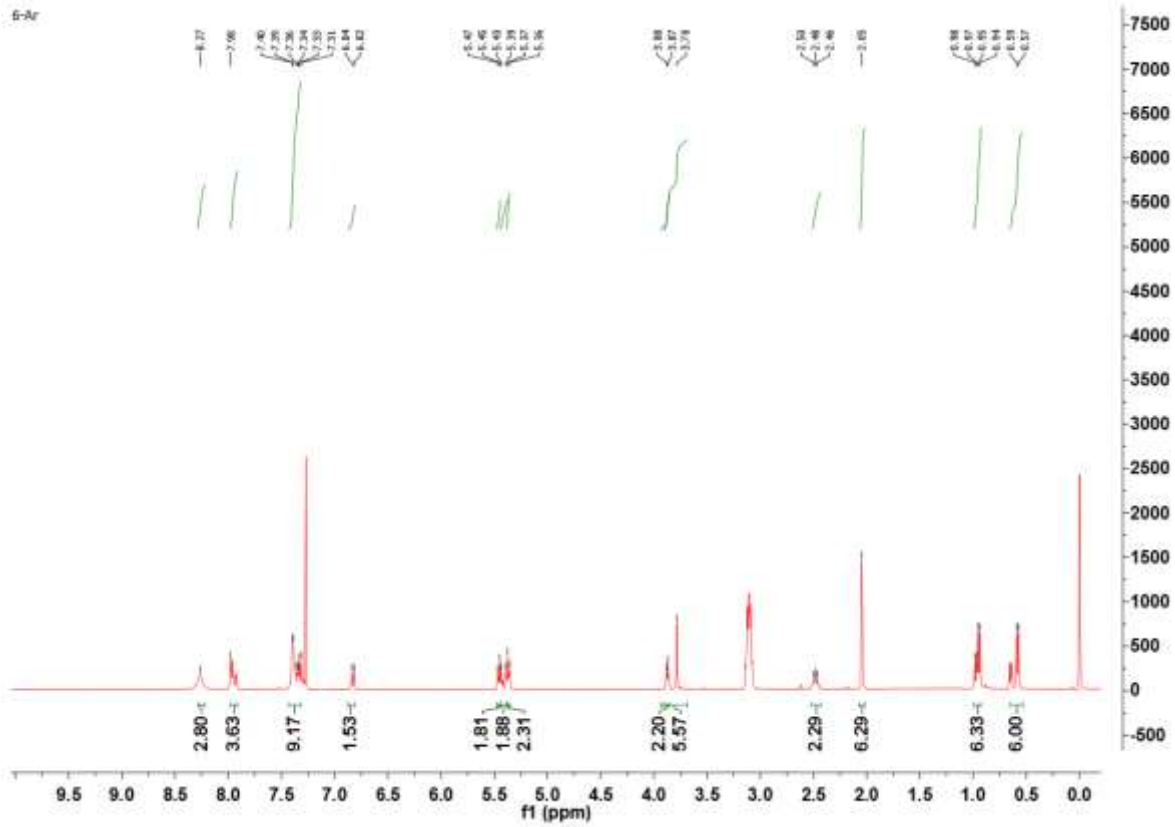

Figure S8. ^{1}H NMR spectrum of [$Ru_2(\eta^6$-p-cymene$)_2(Cl)_2$(L3)] (**6**) in $CDCl_3$ at 400 MHz.

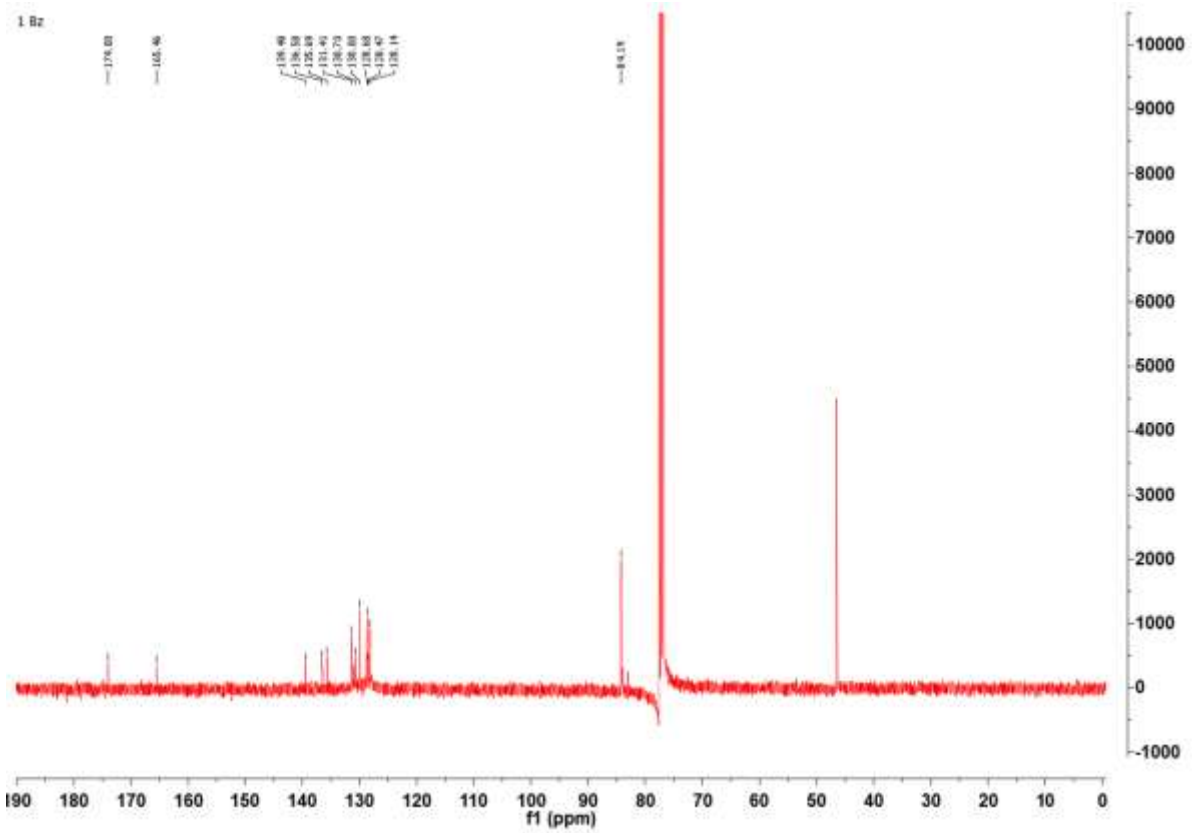

Figure S9. $^{13}C\{^{1}H\}$ NMR spectrum of $[Ru_2(\eta^6\text{-}C_6H_6)_2(Cl)_2(L1)]$ (**1**) in $CDCl_3$ at 100 MHz.

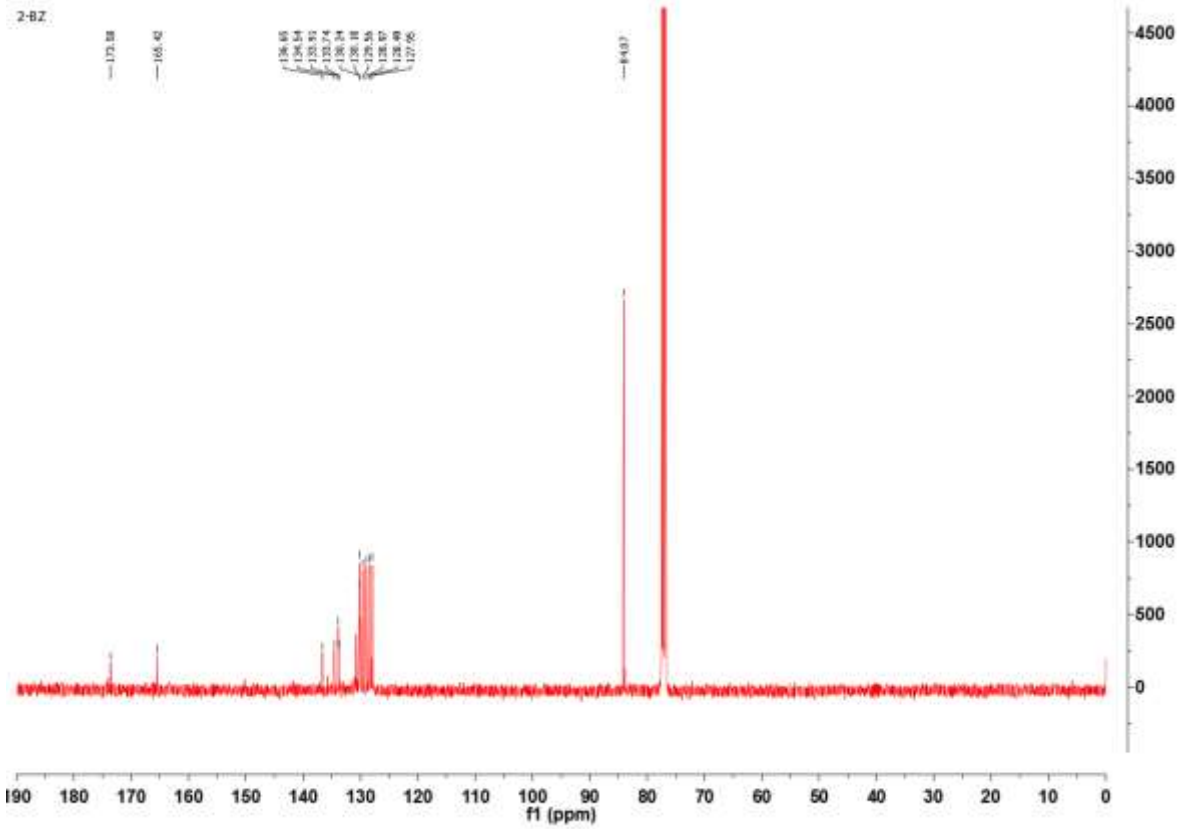

Figure S10. $^{13}C\{^{1}H\}$ NMR spectrum of $[Ru_2(\eta^6\text{-}C_6H_6)_2(Cl)_2(L2)]$ (**2**) in $CDCl_3$ at 100 MHz.

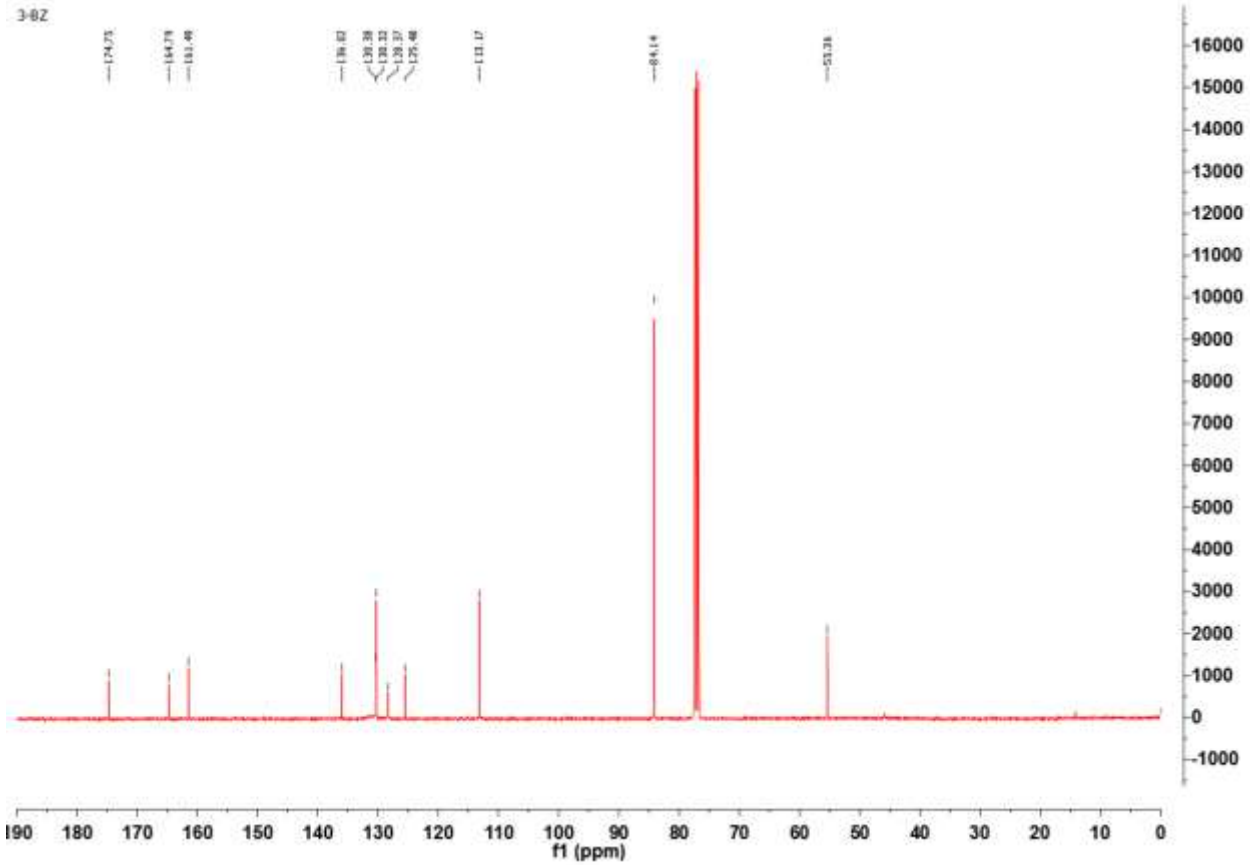

Figure S11. $^{13}C\{^{1}H\}$ NMR spectrum of $[Ru_2(\eta^6\text{-}C_6H_6)_2(Cl)_2(L3)]$ (**3**) in $CDCl_3$ at 100 MHz.

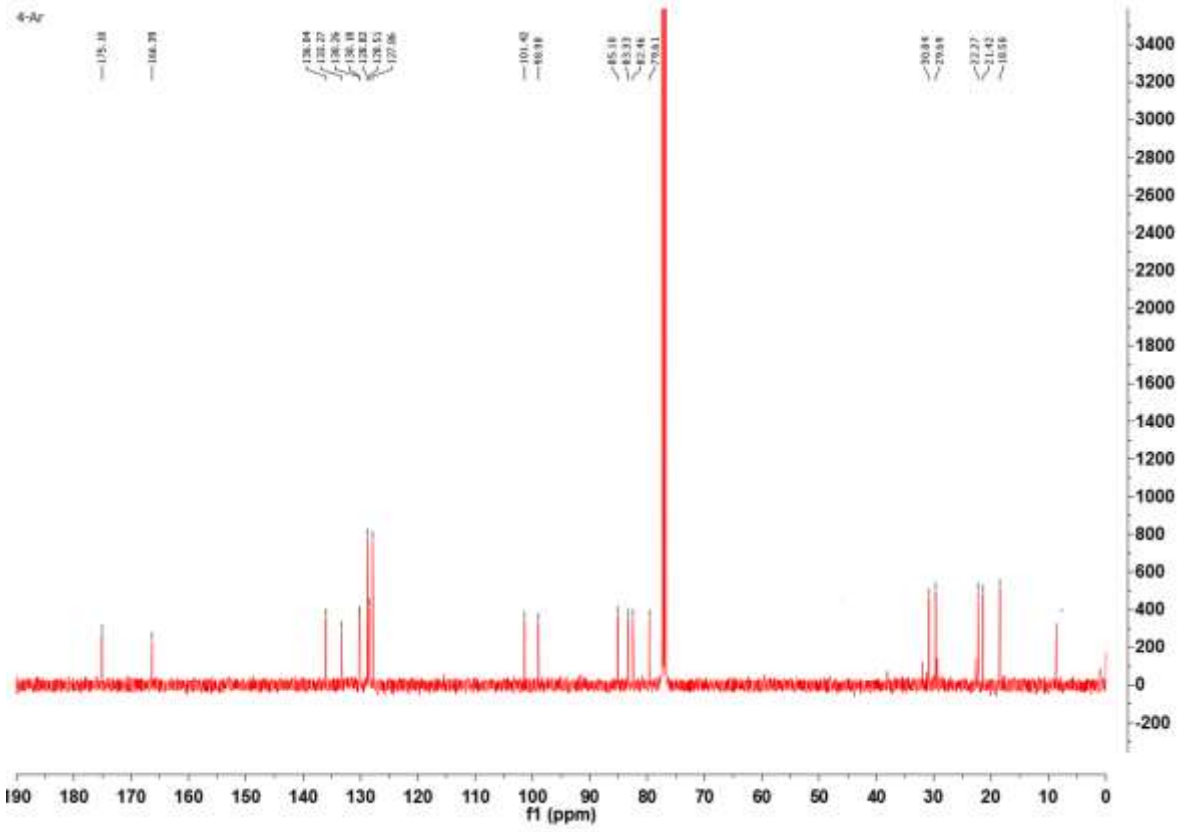

Figure S12. $^{13}C\{^{1}H\}$ NMR spectrum of $[Ru_2(\eta^6\text{-p-cymene})_2(Cl)_2(L1)]$ (**4**) in $CDCl_3$ at 100 MHz.

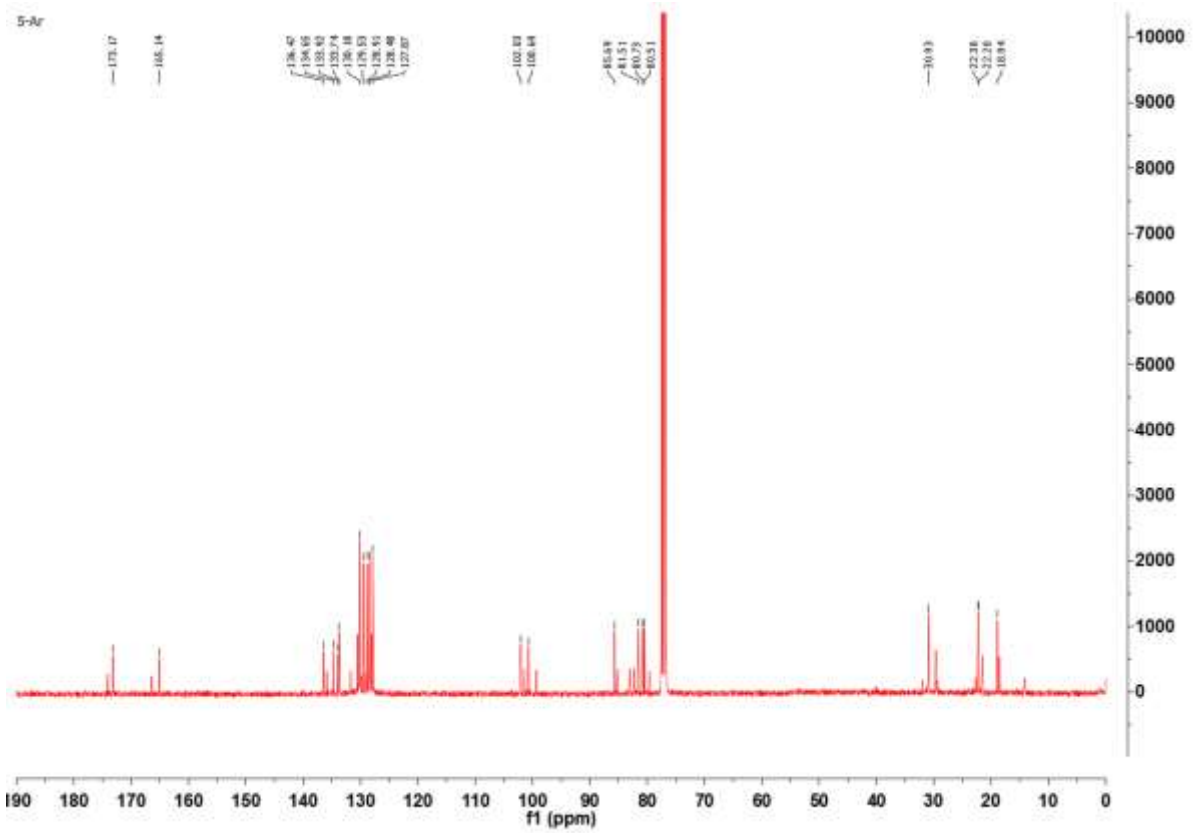

Figure S13. $^{13}C\{^{1}H\}$ NMR spectrum of $[Ru_2(\eta^6\text{-p-cymene})_2(Cl)_2(L2)]$ (**5**) in $CDCl_3$ at 100 MHz.

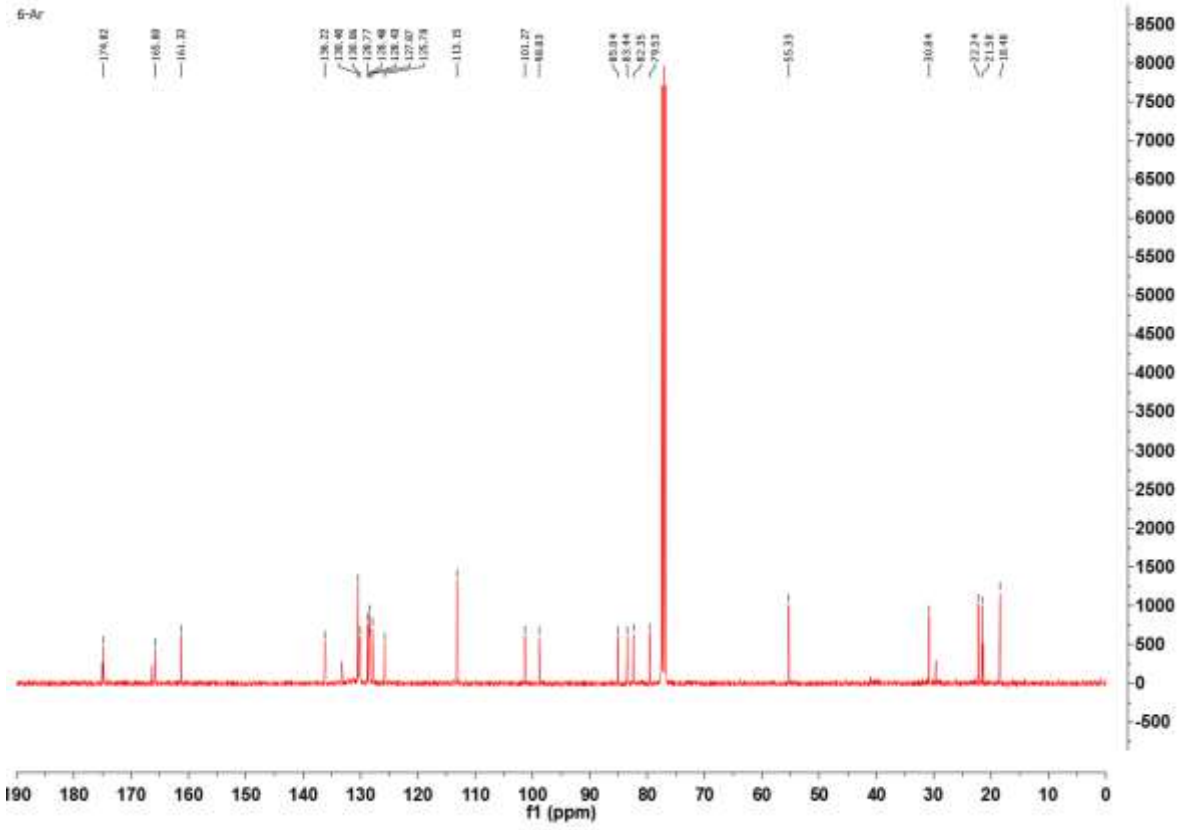

Figure S14. $^{13}C\{^{1}H\}$ NMR spectrum of $[Ru_2(\eta^6\text{-p-cymene})_2(Cl)_2(L3)]$ (**6**) in $CDCl_3$ at 100 MHz.

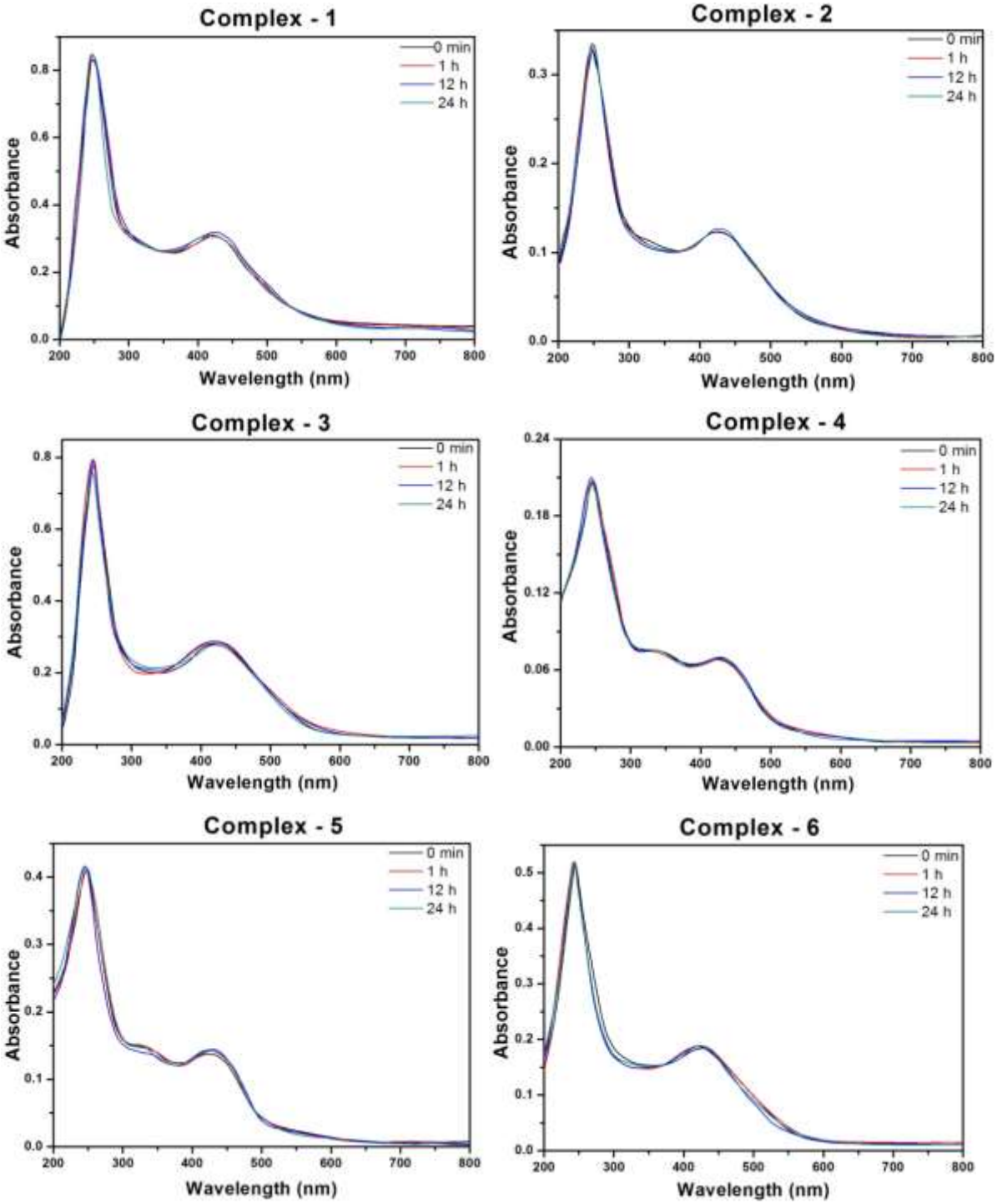

Figure S15: Stability studies of the complexes **1-6** in 1% DMSO in PBS solution.

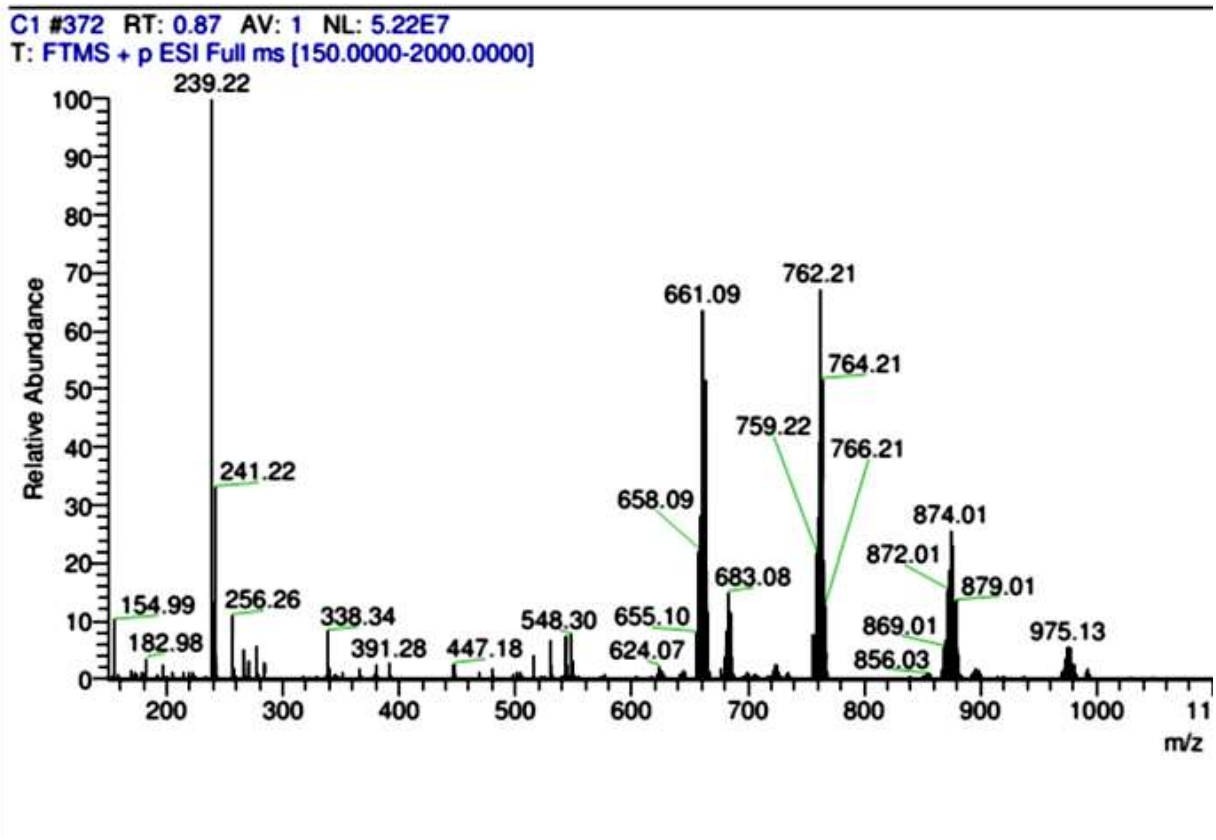

Figure S16: ESI-Mass spectrum of $[Ru_2(\eta^6\text{-}C_6H_6)_2(Cl)_2(L1)]$ (**1**).

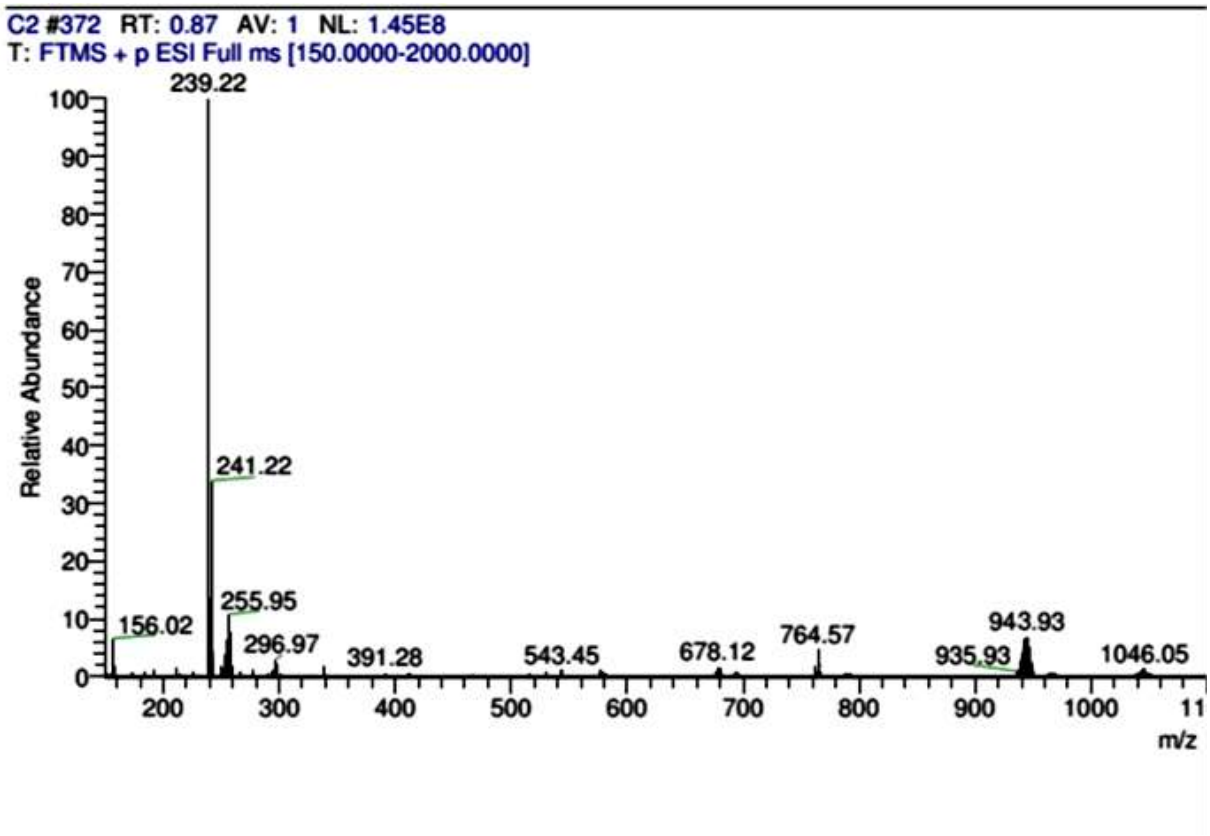

Figure S17: ESI-Mass spectrum of $[Ru_2(\eta^6\text{-}C_6H_6)_2(Cl)_2(L2)]$ (**2**).

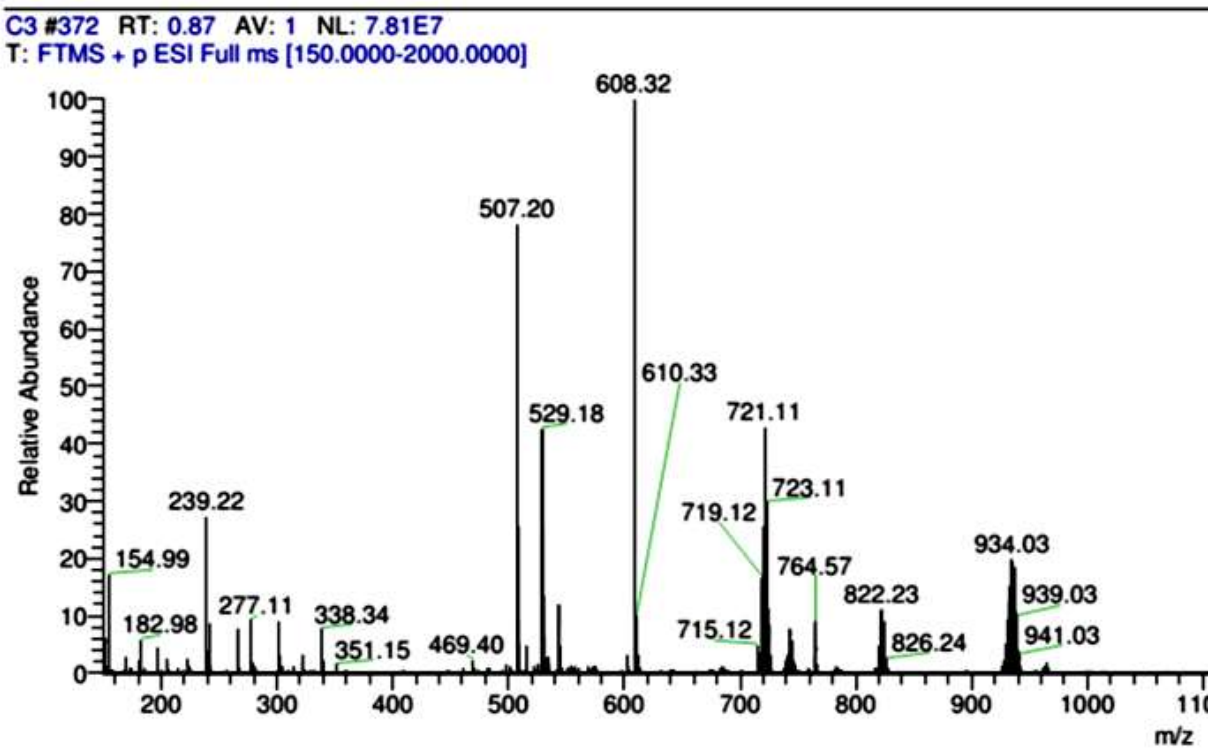

Figure S18: ESI-Mass spectrum of $[Ru_2(\eta^6\text{-}C_6H_6)_2(Cl)_2(L3)]$ (**3**).

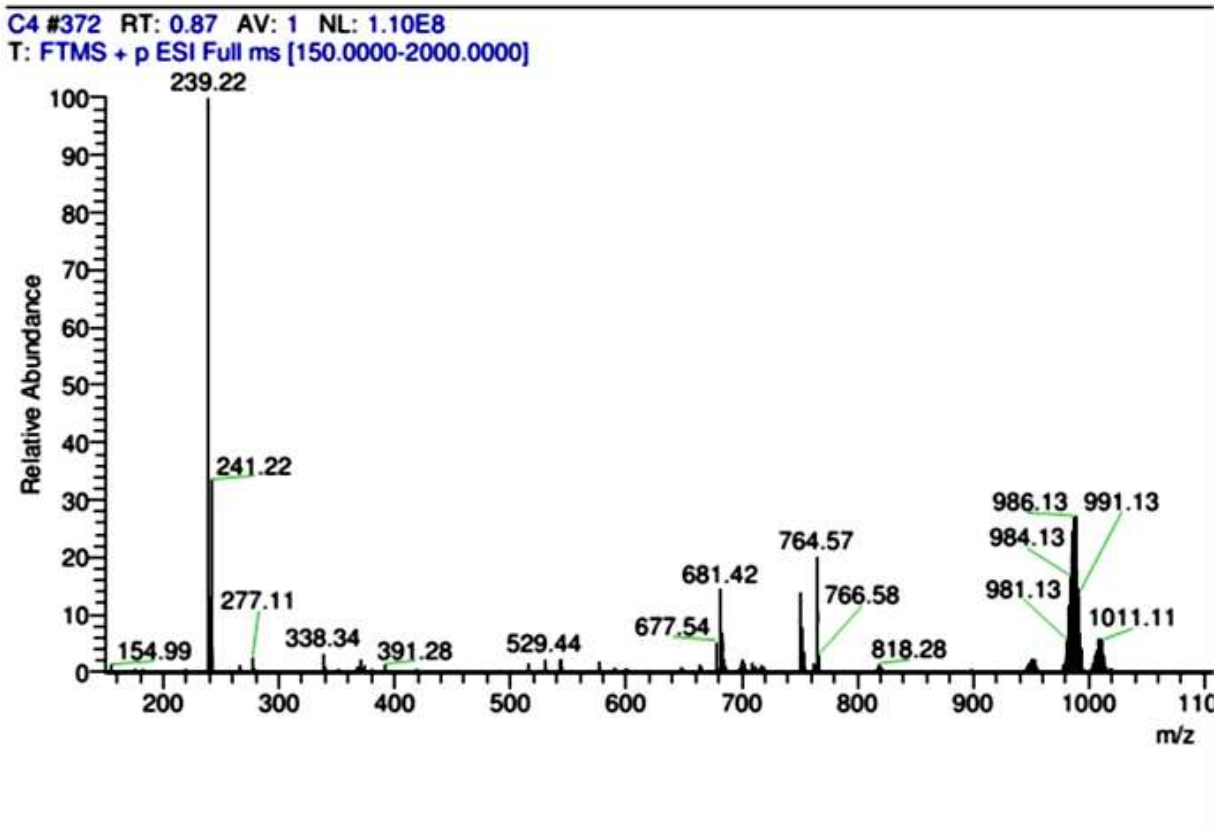

Figure S19: ESI-Mass spectrum of $[Ru_2(\eta^6\text{-p-cymene})_2(Cl)_2(L1)]$ (**4**).

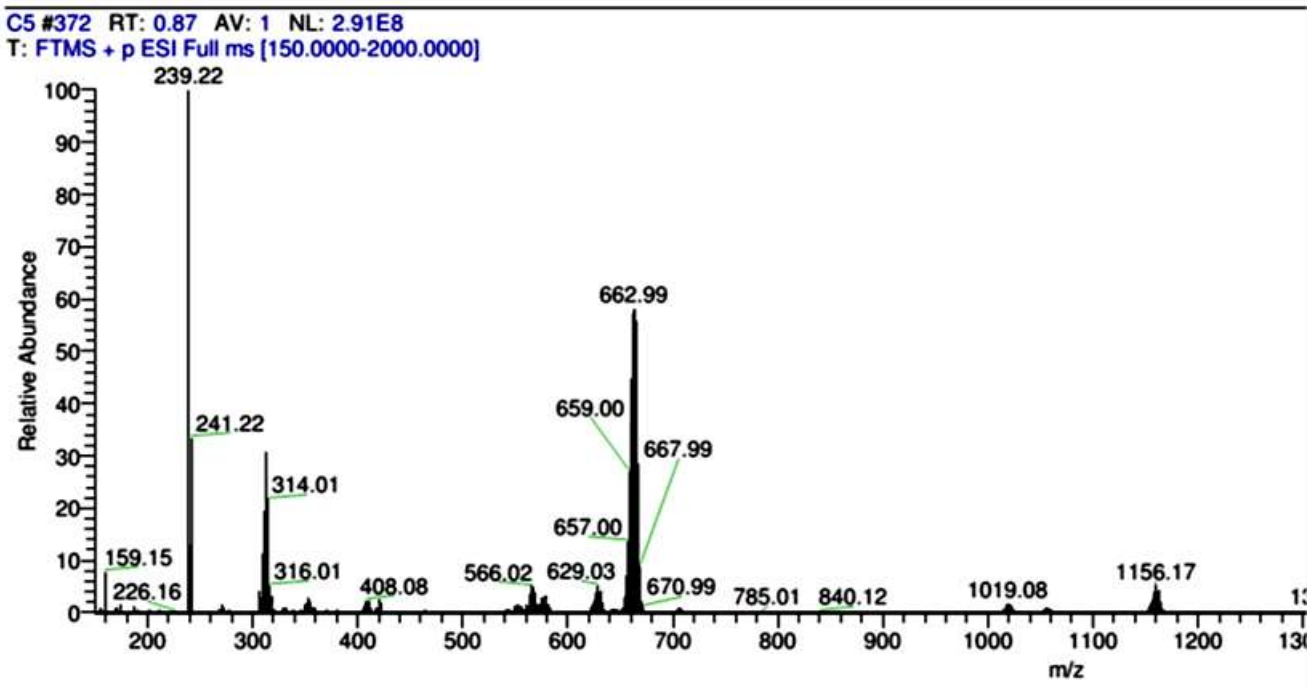

Figure S20: ESI-Mass spectrum of $[Ru_2(\eta^6\text{-p-cymene})_2(Cl)_2(L2)]$ **(5).**

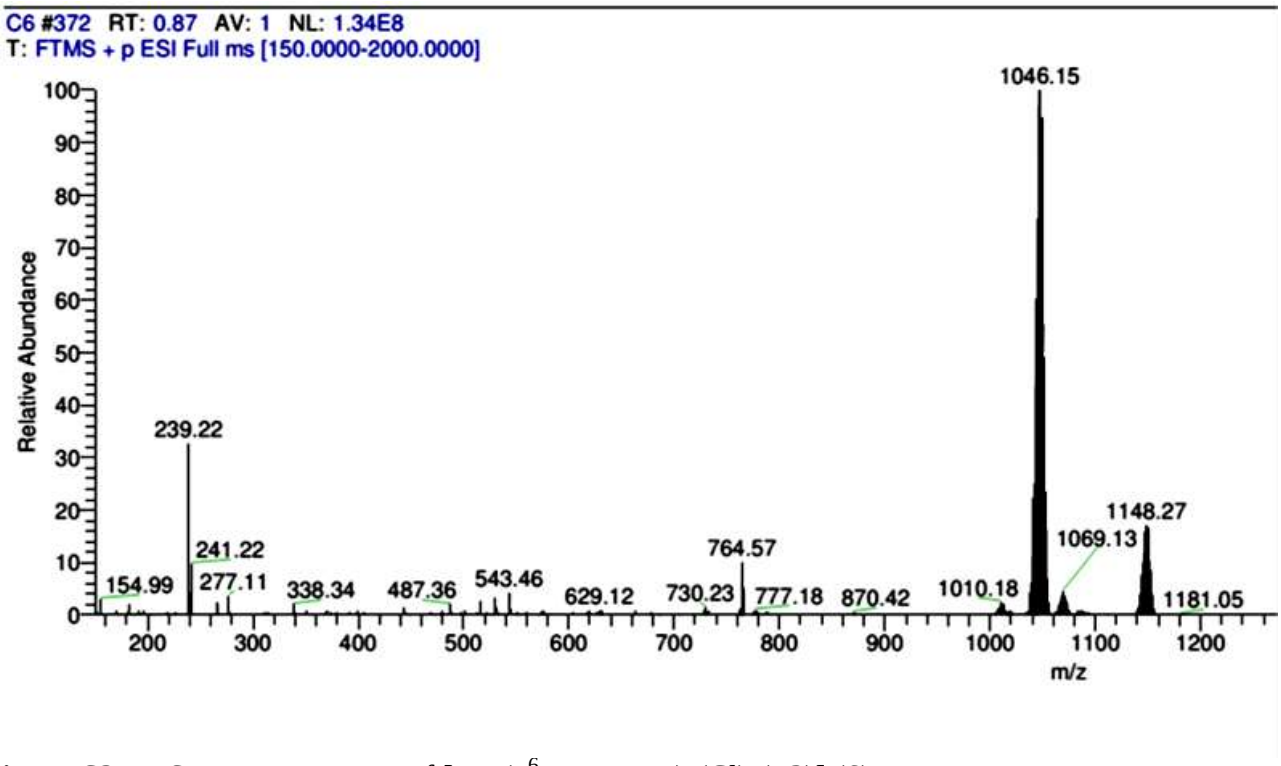

Figure S21: ESI-Mass spectrum of $[Ru_2(\eta^6\text{-p-cymene})_2(Cl)_2(L3)]$ (**6**).

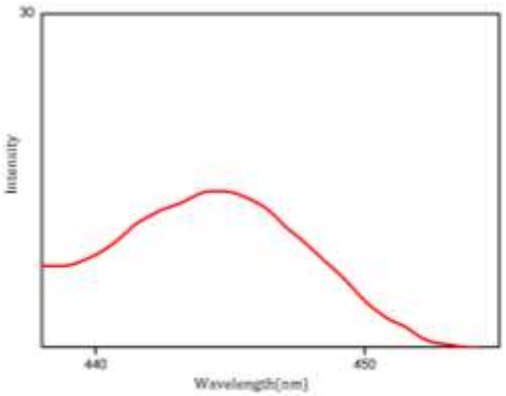

Figure S22. Emission spectrum of complex **(4)**.